Reliability Engineering and System Safety 212 (2021) 107614

Contents lists available at ScienceDirect

Reliability Engineering and System Safety

journal homepage: www.elsevier.com/locate/ress

A fault detector/classifier for closed-ring power generators using machine learning

Igor M. Quintanilha [a], Vitor R.M. Elias [a], Felipe B. da Silva [a], Pedro A.M. Fonini [a], Eduardo A.B. da Silva [a], Sergio L. Netto [a], José A. Apolinário Jr. [b], Marcello L.R. de Campos [a,*], Wallace A. Martins [a,d], Lars E. Wold [c], Rune B. Andersen [c]

[a] Electrical Engineering Program, COPPE/Federal University of Rio de Janeiro, Brazil
[b] Department of Electrical Engineering at the Military Institute of Engineering, Brazil
[c] Siemens Norge AS, Oslo, Norway
[d] Interdisciplinary Centre for Security, Reliability and Trust, University of Luxembourg, Luxembourg

ARTICLE INFO

Keywords:
Condition-based monitoring
Detection
Classification
Machine learning
Principal components
Random forests

ABSTRACT

Condition-based monitoring of power-generation systems is naturally becoming a standard approach in industry due to its inherent capability of fast fault detection, thus improving system efficiency and reducing operational costs. Most such systems employ expertise-reliant rule-based methods. This work proposes a different framework, in which machine-learning algorithms are used for detecting and classifying several fault types in a power-generation system of dynamically positioned vessels. First, principal component analysis is used to extract relevant information from labeled data. A random-forest algorithm then learns hidden patterns from faulty behavior in order to infer fault detection from unlabeled data. Results on fault detection and classification for the proposed approach show significant improvement on accuracy and speed when compared to results from rule-based methods over a comprehensive database.

1. Introduction

Dynamic positioning (DP) is used in vessel stabilization when anchoring is not feasible, or desirable, e.g., in floating drilling platforms. It is a well established primary method for vessel positioning, particularly in deep water applications [1]. DP is performed by automatically controlling propellers and thrusters according to various sensor measurements related to the vessel position [2]. As positioning is crucial and greatly dependent on power availability and on the proper operation of propellers and thrusters, faults that affect the DP system are critical. For this reason, the Maritime Safety Committee issued guidelines for international operation of DP vessels [3], establishing that a DP3-class vessel shall not lose position in the event of a single fault in any active or static component.

Failures in power-generation systems can be catastrophic, and their effects are often mitigated with comprehensive protection systems that involve redundancy [4] and condition monitoring [5–7]. Although the two strategies are expected to work in tandem, modern system designs, such as closed-ring power systems [8], tend to rely more on the protection offered by condition-based monitoring and less on the expensive and inefficient use of fallback spare parts [9]. Improved reliability in redundant systems comes at the cost of increased capital and operating expenses, decreased efficiency, and large footprint. If good monitoring is available, autonomous and automatic reaction can quickly set off alarms, isolate the problem, and prompt the system for further action. Moreover, employing a reliable autonomous system reduces the actuation-error probability when a human operator is present [10]. In this context, this work proposes a *machine-learning* (ML) *condition-based monitoring* (CBM) solution for ancillary fault detection and classification in power-generation systems of DP-based vessels.

DP vessels generally have an on-board power plant which produces the electrical energy required to feed DP-related equipment. The basic power-generation structure used is a triad composed of an electric generator, a combustion engine, and an *automatic voltage regulator* (AVR) [11,12]. A power plant may contain multiple power-generation blocks with properly coupled digital sensors capable of measuring signals related to several mechanical and electrical variables. Traditional rule-based protection systems employ a combinatorial logic from these

* Corresponding author.
E-mail addresses: igormq@poli.ufrj.br (I.M. Quintanilha), vtrmeireles@poli.ufrj.br (V.R.M. Elias), fbs@poli.ufrj.br (F.B. da Silva), fonini@poli.ufrj.br (P.A.M. Fonini), eduardo@smt.ufrj.br (E.A.B. da Silva), sergioln@smt.ufrj.br (S.L. Netto), apolin@ime.eb.br (J.A. Apolinário Jr.), campos@smt.ufrj.br (M.L.R. de Campos), wallace.martins@smt.ufrj.br (W.A. Martins), lars.erik.wold@siemens.com (L.E. Wold), rune.b.andersen@siemens.com (R.B. Andersen).

https://doi.org/10.1016/j.ress.2021.107614

Available online 26 March 2021

variables and judiciously chosen thresholds to set off an alarm in the event of a hazard. In contrast, ML techniques can learn hidden patterns from data enabling detection and classification of abnormal operation.

In order to address power-system faults, many techniques have been considered, which may involve vibration and acoustic detection, electrical measurements, and a posterior analysis of these characteristics. Among the methods for such analysis, three of them can be mentioned, viz.: (i) rule-based approach; (ii) signal processing approach; and (iii) ML approach. The first one relies on physical and theoretical knowledge about the system, is highly dependent on the particular implementation, and usually does not cope well with changes in parameters. A range of techniques can be found in the literature for fault detection, location, and classification in different segments of power generation/distribution systems [13,14]. For instance, a rule-based methodology that tracks voltage displacement is proposed in [15]. With a similar approach, [16] uses cumulative sums to improve resilience to noise. In [17], the authors present a real-time method for detection of faults in frequency control loops based on robust fault detection filter (RFDF) design, whereas in [18], the method relies on the voltage level to detect open circuit faults in insulated-gate bipolar transistors (IGBT).

Signal-processing-based approaches may employ, e.g., discrete wavelet transform (DWT) [19], as used in [7] for CBM of steam turbine generators. Observer residuals are used for fault detection in different scenarios, such as manufacturing machinery [20], and in photovoltaic power generation systems [21,22]. Residuals are also employed in [23] using a graph-based modeling approach for fault detection and location in power systems. Another signal-processing tool commonly employed to analyze power-system signals and detect and diagnose possible faults is the principal component analysis (PCA) [24,25]. These methods may offer increased robustness to noise and better signal visualization, which can enhance results. In [26], non-technical losses in power systems are detected using DWT combined with random undersampling boosting. In [27], faults are located in large power networks using a small number of sensors and a constrained compressed sensing method. The work in [28] proposes a modular approach allowing for the use of different techniques, such as multirate signal processing, residuals monitoring, and artificial neural networks (ANN).

ML techniques are more data-driven, if compared to the aforementioned methods, and the system parameters are learned in an initial training stage. Several ML-based algorithms are suitable for the task of fault detection and their applications can be found in the literature [29–35]. In [6], a variety of ML-based methods are employed and compared in the CBM of naval propulsion systems. Additionally, we may cite, e.g., ML-based works which use support vector machine (SVM) to detect line-to-line faults in photovoltaic arrays [34] and to classify anomalies in the systems of a nuclear power plant [35]. Deep learning (DL) architectures are employed to detect and classify faults in high-voltage applications [36] and in hydraulic pumps [37]. A generic framework for DL-based CBM and failure prognostics is presented in [38]. Nonetheless, DL techniques require a huge amount of data to train the models properly, which is not always feasible. Other applications of fault detection methods based on ML found in the literature include ANN [39,40] and self-organizing maps [41]. The works in [32,33] propose ML-based approaches for fault detection in medium-voltage direct current shipboard power systems. We note that this work uses a three-phase alternating current system.

Our approach consists of using the random forest (RF) [42–44] algorithm, which does not require as much data as DL, yet yields solid detection and classification results. For condition monitoring of DP vessels, there are works using neural networks to model diesel engines and predict faults using rule-based approaches [45], and those focusing on ML techniques to detect faults on control systems [46]. In [47], the authors propose an electrical system fault simulator in order to investigate new power plant control strategies and new power sources, whereas [48] focuses on the design of such systems. However, to the best of our knowledge, none aims to detect and classify faults in closed-ring power systems of DP vessels using the RF technique. This application is particularly important as DP3-class vessels have increased safety requirements, and can readily benefit from the advantages of ML techniques.

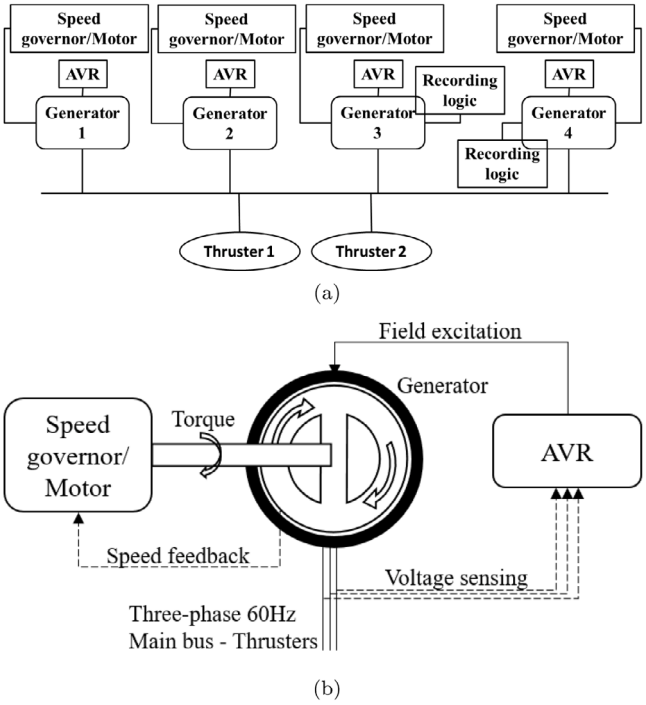

Fig. 1. Engine-room diagrams employed in our experiments: (a) two thrusters shared by four generators. Each generator is fed by an AVR and a diesel engine simulator (speed governor and motor); (b) details of the connections between generator, motor, and AVR, and some relevant signals for the proposed methodology.

In this work, we target the detection and classification of 12 types of faults that may occur in power-generation systems used in DP vessels. These systems differ from those in conventional vessels by having increased redundancy, leading to several generators connected in a configuration that allows for fault isolation, in order to deliver a reliable power supply. We show the usefulness of artificial intelligence algorithms for achieving faster response time and, consequently, increased situational awareness against traditional protection methods. We also provide information on feature relevance for the detection of different faults. For comparison purposes, we use a *generator performance controller* (GPC) developed by Siemens to protect electrical power systems for DP3-class operations [49].

2. Energy-generation and protection systems

In a redundant system, engine rooms usually comprise at least two electric generators, along with their corresponding combustion engines and AVRs. In the three-phase power-generation system considered in this work, the load is shared among four generators running simultaneously, as illustrated in Fig. 1.

2.1. Fault description

A total of 12 different types of anomalies are considered here. These faults correspond to predefined scenarios tackled by the previous protection system, the GPC, and were kept to allow comparison between methodologies. They are grouped as AVR-related faults (T01 to T06) and engine-related faults (T07 to T12), despite the fact that they may occur due to internal errors in these blocks, or due to problems in the feedback system [9,50]. Relevant interconnections between the generator and the AVR, and between generator and speed governor (engine) are depicted in Fig. 1b.

T01 — loss of voltage sensing. The voltage sensing, which serves as a feedback for the AVR, is lost for the three phases. This results in an AVR over-excitation, as its control system tries to compensate for the detection of a zero-valued voltage at the generator output.

T02 — internal AVR fault. It is caused by internal AVR issues, resulting in incremental steps of over-excitation.

T03 — non-functioning AVR. In this fault, the AVR stops providing excitation current for the generator.

T04 — faulty AVR gain. This fault results from an improper gain design for the proportional–integral–derivative (PID) controller inside the AVR [51,52], which causes oscillations on the excitation signal around its reference level.

T05 — faulty AVR derivation gain. It arises from an improper design of the derivation gain for the PID controller inside the AVR, also causing oscillations on the excitation signal.

T06 — partial loss of voltage sensing. This fault is associated with a single wire breaking, resulting in zero-valued feedback from one of the three generator phases, yielding over-excitation, similar to T01.

T07 — loss of speed sensing. In this fault, the speed sensing, which serves as a feedback for the engine's governor [12], is completely lost, yielding over-production, forcing the diesel engine to work at full-power.

T08 — overproduction. This fault is usually caused by problems in the fuel actuator [53], which may get stuck in an overproduction position, resulting in oscillations in the generator's output frequency.

T09 — underproduction. Similarly to T08, this fault is usually caused by problems in the fuel actuator, which may get stuck in an underproduction position, also resulting in oscillations in the generator's output frequency.

T10 — non-functioning speed controller. In this faulty scenario, the speed controller stops working and the corresponding engine ceases to provide mechanical power to the generator's rotor.

T11 — faulty speed controller. In this fault, a high derivation gain in the PID device inside the speed controller causes oscillations in the engine's output.

T12 — frozen fuel rack. Similarly to T08 and T09, this fault occurs when the fuel rack that dictates the fuel flow to the diesel engine gets stuck.

2.2. Traditional protection system

In the rule-based protection mechanism developed for this application, the generator performance controller [49] (GPC) is divided into two levels with separated logics, namely GPC level 1 and GPC level 2, which are responsible for performance control over the AVR and the diesel engine, respectively. These logics are composed of sets of rules whose inputs are analog signals observed in the power-generation system. These rules are based on thresholds that once compared to the values of the observed signals would trigger, as output of the GPC, a detection flag for one of the 12 fault types. The rules may also consider signals that are not directly observed, but can be derived from those. Examples of directly observed signals are three-phase voltage and current signals, and of non-directly observed signals are estimated frequency and power factor.

2.3. Fault-detection via machine learning

Different CBM approaches may be considered in practice, ranging from methods built upon human knowledge to methods completely based on artificial intelligence. At the human-knowledge end lies the most intuitive CBM idea, in which an expert analyzes an equipment through sensor signals and determines its current operating condition based on his/her professional experience. Halfway through the CBM spectrum, one can find the rule-based methods such as the one implemented by the GPC (see Section 2.2). These methods, despite still relying on human knowledge to create the rules, are automatically executed.

In this work we propose an approach heavily based on supervised ML methods, that are composed of two stages: training and inference. In this scenario, the RF algorithm was chosen due to its low complexity, simple tuning, and good generalization capabilities [42,54]. The ensemble learning [55,56] method employed by the RF algorithm carries most of the advantages from decision trees [57–60], such as being able to handle several types of input without requiring intensive data preparation, and the ability to provide evidence of feature importance. Each decision tree inside an RF algorithm yields a probability for each of the possible labels for a given input. By using the outputs of several independent decision trees, the RF generates a probability for each label, thus avoiding overfitting an improving stability and robustness to data variation.

3. Database development

3.1. Data acquisition

The database employed in this work was collected from real experiments in a laboratory used for simulating a large scale power-generation system of a dynamically-positioned vessel. The lab equipment consists of a test room with four generation blocks (G1 to G4) and two thrusters, as seen in Fig. 1. Each generation block is composed of an electric generator, an AVR, and a diesel engine simulator. The thrusters represent the system load. Two of the generators, namely generators G3 and G4, are equipped with an individual protection system comprised of a relay with a programmable logic controller (PLC) where fault-detection and signal-recording logics are implemented. This system provides the rule-based solution against which we compare the proposed ML-based CBM.

Each of the faults presented in Section 2.1 was introduced separately in the system. Automatic recording took place only when a fault was detected by the rule-based GPC. Manual recording was employed otherwise. The total duration of the recording could be set up to at most 80 s.

Five different configurations were considered for each fault. Faults were induced on a single generator, chosen randomly between G3 or G4, but signals were recorded on both generators. The load L was adjusted by setting the speed of the thrusters, therefore real power ratings may have small deviations from the values given below:

- Configuration 1: Running G3 & G4 with $L = 0\%$ with no thruster connected;
- Configuration 2: Running G3 & G4 with $L = 25\%$ with thruster 2 connected;
- Configuration 3: Running G3 & G4 with $L = 50\%$ with thrusters 1 and 2 connected;
- Configuration 4: Running G2 & G3 & G4 with $L = 0\%$ with no thruster connected;
- Configuration 5: Running G1 & G2 & G3 & G4 with $L = 35\%$ with thrusters 1 and 2 connected.

From the 120 sets of signals (from 2 generators, with 5 different configurations, for 12 faults), 115 were successfully collected. For T09, only data from the faulty generator could be collected using automatic recording. Given time constraints, T09 was not recorded using manual recording, thus five sets of signals are missing. Moreover, additional data were recorded for T01: for each of the five T01 configurations, five slightly different sub-experiments were considered, in which the power rating was increased in steps of 5%. In addition, in order to simulate the effects of sea waves on thrusters, four normal-operation recordings were conducted with the load varying according to a sine wave. These yielded 48 extra sets of signals, leading to a total of 163 sets. Signals were recorded in the COMTRADE (IEEE Std C37.111-1999) file format [61].

For the specific problem treated in this work, the generator's signals usually consisted of an initial segment where the system was working properly, with no fault. At a given instant, referred to as *fault onset* and labeled *onset*, a fault was introduced. After the fault onset, there is a transient period preceding the stabilization at a faulty steady state. The stabilization instant is referred to as *fault stabilized* (labeled *stable*). Not every fault type has a well-defined stabilization instant, so the *stable* label is used to indicate the end of the first transient period, which is defined, for instance, by the first signal overshoot or knee region after the beginning of the fault. The third (and last) relevant time instant is when the fault cause is turned off, referred to as *fault end* or *fault offset*.

Given these three time instants, each signal was divided into three parts: healthy steady state, fault transient, and faulty steady state. For each signal the fault type was known, but the exact time instants when the fault was introduced, or stabilized, was unknown. Therefore, labeling was carried out manually by visual inspection of the waveforms. This process was performed independently by four different people. For each labeled time instant, the four instances were compared, and any outliers caused by human error during visual labeling were relabeled. This process was repeated until the standard deviation of the four instances was significantly less than the duration of the fault transient.

3.2. Data analysis

For each generator, 18 sensor measurement signals, listed in Table 1, were recorded. These are mainly three-phase plus neutral current and voltage signals acquired at the generator, the speed-governor output, and the AVR output, all driven by the same clock.

The sampling frequency was set to 2 kHz during the data-processing phase. All acquired time series were *windowed*, that is, each signal was divided into segments of a given number of samples. From these raw windowed data, features were calculated, extracting relevant statistical and physical information.

For each of the 18 signals in Table 1, the following nine statistical features were calculated from each data segment: minimum value (min); maximum value (max); first quartile; median; third quartile; mean; standard deviation (std); skew; kurtosis. Additionally, 10 other features that carry physical information about the system were also employed: active power; derivative of active power; reactive power; derivative of reactive power; apparent power; frequency; derivative of frequency; power factor; RMS voltage; derivative of RMS voltage. All derivatives were computed with respect to values from the previous segment. The above process yields a total of 172 features (9 statistical features for each of the 18 signals + 10 overall physical features) per data segment.

Large redundancy among different features has been observed and, in order to deal with such redundancy, *principal component analysis* (PCA) was used [62,63]. PCA is a mathematical procedure that decorrelates data; it uses an orthogonal transformation to project the original highly-correlated data into a set of sample-wise orthogonal variables called *principal components*. After the transformation, the information that is spread along many of the correlated features becomes concentrated in few principal components, allowing dimensionality reduction.

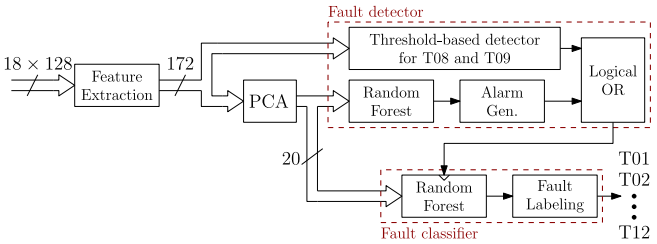

Fig. 2. Block diagram of the complete ML-based procedure.

The *explained variance* is a measure of how much a given principal component contributes to the total data variance. By applying the PCA to our 172-feature dataset, 99.7% of the total variance is concentrated in only 20 principal components, which then become the input to the random-forest fault classifier described in the next section. The principal components carry information about all features, as opposed to other feature-selection methods, such as selecting the top-ranked features from the RF algorithm.

4. Fault detection/classification methodology

The first step in building the proposed fault detection system was to process and prepare the data for the ML training. In this process, for each generator, the 18 signals labeled as relevant in Table 1 were selected. From each of those signals, associated with the several sensors and represented as time series with 2000 samples per second, data segments of $w = 128$ samples were generated. In this work, we used sliding windows, i.e, consecutive windows having an overlap of $w - 1 = 127$ samples (*hop size* equal to only $h = 1$ sample). For each synchronized set of 18 segments, 172 features were extracted and used as the input for the *fault detector* block in Fig. 2.

When preparing data to train the ML model, we used only a portion of the signal closest to the *onset* label, namely the 5000 samples immediately before and the 5000 samples immediately after the *onset*. After the *onset*, there is a transient period in which signals change from a steady normal operation to a steady faulty operation. Using data from the steady faulty operation for training tends to worsen detection results, as samples may look healthy, but are marked as faulty, which tends to increase the number of false detections. In addition, using data predominantly from the beginning of the fault is not detrimental, because in practice the algorithm should detect the fault before the system reaches the steady faulty operation. In cases where faults have a slow transient, it is expected that healthy and early faulty samples are similar, which can result in slower detection.

The model proposed in this work, as given in Fig. 2, consists of two main ML stages, designated as *fault detector* and *fault classifier*. Considering that detecting a fault is simpler than categorizing it among the 12 fault types under consideration, the main objective of the fault detector is just to provide a *fault* or *not-fault* flag.

4.1. Fault detector

As also shown in Fig. 2, the fault detector developed in this project is composed of two sub-detectors. The alarm indicating a fault is set off if either of the outputs of the sub-detectors indicates the occurrence of a fault. The RF algorithm employed in the ML-based sub-detector provides a fault probability according to the trees' outputs for each input sample, whereas the rule-based sub-detector provides a binary output of *fault* or *not-fault*. An *alarm generation* block, comprised of two simple operations, namely *calibration* and *voting*, was inserted after the RF model to make it binary and also to take into account its inherent temporal structure.

Since the T08 and T09 faults can be detected by a simple rule-based model on the reactive power and frequency signals, these faults were

Table 1
Relevant signals from the test room data.

Comtrade name	Description
Line CT (-T1 & -T90):I A	Switchboard current transformator phase A for generator
Line CT (-T1 & -T90):I B	Switchboard current transformator phase B for generator
Line CT (-T1 & -T90):I C	Switchboard current transformator phase C for generator
Line CT (-T1 & -T90):IN	Switchboard current transformator phase Neutral for generator
Busbar VT (-T15):V A	Switchboard voltage transformator phase A for Busbar
Busbar VT (-T15):V B	Switchboard voltage transformator phase B for Busbar
Busbar VT (-T15):V C	Switchboard voltage transformator phase C for Busbar
Busbar VT (-T15):VN	Switchboard voltage transformator phase Neutral for Busbar
Gen CT (-T10 & -T91):I A	Generator current transformator phase A (stator)
Gen CT (-T10 & -T91):I B	Generator current transformator phase B (stator)
Gen CT (-T10 & -T91):I C	Generator current transformator phase C (stator)
Gen CT (-T10 & -T91):IN	Generator current transformator phase Neutral (stator)
Line VT (-T5):V A	Switchboard voltage transformator phase A for generator
Line VT (-T5):V B	Switchboard voltage transformator phase B for generator
Line VT (-T5):V C	Switchboard voltage transformator phase C for generator
Line VT (-T5):VN	Switchboard voltage transformator phase Neutral for generator
Analog units:MT fast:Governor output:	Speed governor output
Analog units:MT fast:Field current:	AVR excitation current

detected separately, improving the RF ability to detect all other faults. The ML-based sub-detector employs an RF algorithm trained with signals related to all but T08 and T09 faults. The RF hyperparameters, such as number of trees and maximum tree depth, were chosen via stratified cross-validation [64]. This process consists in splitting the training set into k smaller sets (folds), ensuring that each fold contains the same number of samples of each fault. After that, the RF model is trained using the set of $k-1$ folds, where the validation set is represented by the remaining fold. Therefore, the hyperparameters are set from the model that achieved the best performance, considering all combinations of training and validation sets, in terms of a predefined metric, e.g., accuracy, and recall.

Since the system can function healthily under different operation points, healthy data from a given operation point can be misinterpreted as a fault on another operation point. Thus, a calibration operation is used to increase the confidence level of the output signal from an ML algorithm [65,66]. This process widens the gap between the probability levels associated with the normal and anomalous operating modes by distorting the fault probability p through a sigmoid function, such that the new probability p' is

$$p' = \frac{1}{1+e^{Ap+B}}, \tag{1}$$

with A and B obtained by minimizing the log-likelihood function for the training dataset [67].

The voting operation is performed after calibration and its function is to make the output of the calibration block binary. It is necessary given the noisy fault probability signal from the calibration output. The voting process occurs within a window containing a sequence of current and past calibration outputs. It counts the number of instances in which the probability is larger than a first fault-probability threshold. Then, it compares this number to a second threshold associated with the number of faulty samples inside a window. These two thresholds are hyperparameters chosen by optimizing the hit rate in the training set using grid-search.

4.2. Fault classifier

The last stage in the proposed system is the *fault classifier*, whose function is to classify the already-detected fault into one of the 12 fault types. It consists of a second RF block, with 12 output classes associated with fault types and trained with faulty data only.

Pre-processing for classification is the same as that used for detection: the system is fed with projections of features over the same 20 principal components. The outputs of the classifier are 12 fault probabilities associated with the 12 types of fault.

5. Experimental results

This section presents the experimental results obtained with the proposed RF-based fault detector/classifier in comparison to the results obtained by the standard GPC logic.

5.1. Fault detection

The original dataset was split into two parts, namely training and testing datasets, using the following procedure: first, the total dataset was divided randomly into 70% of the overall data for training and 30% for testing. Due to the imbalance among faults, these sets were stratified, which means that the proportion (70, 30)% is guaranteed for every fault. The training data were further reduced so that each fault was represented by only three experiments, whereas the remaining training data were then used for calibration. For cross-validation, we set $k = 3$ folds, and employed the Cohen-Kappa [68] metric to evaluate their performance. The voting procedure used windows of 180 samples and a vote in favor of a fault was counted when the calibrated probability, defined in Eq. (1), was larger than 0.4. The alarm was triggered if at least 108 votes equal to one were counted for each data segment.

Results from the testing dataset are summarized in Table 2, comparing the proposed method against the rule-based algorithm used in the GPC. Table 2 also shows the total number of detection problems (either false alarm or miss detection) that occurred when using the proposed system and the GPC.

The detection results may be summarized as follows:

- T01 was the fault case with the most testing data available, with a total of 20 generator recordings (10 from healthy + 10 from faulty generators). For most cases, the proposed detector outperformed the GPC logic. Four false alarms occurred in the proposed system for this fault.
- For T02, there were two experiments and four generators available for tests. For this fault, the proposed detector was considerably faster than the GPC logic and no detection errors occurred.
- There was only one experiment for testing T03, with recordings for two generators. The GPC was not able to detect the fault. So T03 was manually recorded, and there was no information about the GPC trigger. Detection was correct and fast.
- Two experiments and a total of four generators were used to test T04. The proposed RF model improved detection when compared to the GPC logic. Detection delays indicated that the fault had a slow dynamic. For one of the generators used in the test, the alarm of the proposed system was triggered before the *onset*.
- T05 was tested with one experiment, composed by the recordings of two generators, for which the proposed detector performed better than the GPC logic.

Table 2
Summary of fault detection results for proposed and GPC systems.

	Total number of signals	Number of problems (proposed)	Number of detections before onset (proposed)	Number of problems (GPC)	Average uncertainty [ms]	Average delay (GPC) [ms]	Average delay (proposed) [ms]	Average interval of detection before onset (proposed) [ms]
T01	20	4 false alarms	–	–	8	**134**	**126**	–
T02	4	–	–	–	85	**6347**	**174**	–
T03	2	–	–	2 misses	8	**–**	**119**	–
T04	4	–	1	–	103	**4242**	**1172**	274
T05	2	–	–	–	78	**5853**	**1043**	–
T06	4	–	–	–	7	**194**	**112**	–
T07	2	–	–	–	34	**159**	**104**	–
T08	4	1 miss	2	4 misses	–	**–**	**8605**	3420
T09	1	–	1	–	–	**1211**	**–**	186
T10	4	–	–	–	157	**2576**	**172**	–
T11	2	–	–	–	13	**8989**	**101**	–
T12	2	1 miss	–	–	439	**15247**	**17449**	–

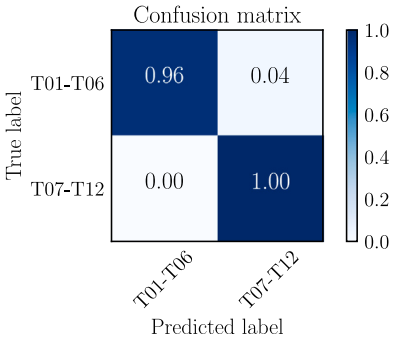

Fig. 3. Confusion matrix for classification considering two groups of faults in Experiment 1: T01–T06 (AVR) and T07–T12 (speed).

- Two experiments and four generators composed the testing database for T06. Detection results were good and fast for both systems, with the proposed system being able to detect T06 faster than the GPC logic.
- For T07, one experiment with two generators was available for testing. Both systems detected the fault correctly, with the proposed system being able to detect T07 faster than the GPC logic.
- Two experiments with a total of four generators were available for testing the detection of T08. The GPC trigger information was not available in this case. The proposed scheme missed the fault for one faulty generator. For the two healthy generators, detection happened before the labeled *onset*, but it must be highlighted that a fault actually occurred before the *onset* label, which marks the sample where reactive power becomes negative. In fact, the rule-based detector for T08 guarantees that if the RF detector misses detection, the trigger will be activated anyway whenever the reactive power becomes negative.
- Only one faulty generator was available for testing T09. Similarly to T08, detection occurred before the *onset*, which corresponds to the instant where reactive power becomes negative. This means that the RF detector is detecting T09 in the same way as T08.
- T10 was tested with two experiments and four generators. Results show that the proposed detector was much faster than the GPC, although the difference in detection delay was not as significant in the faulty generators.
- One experiment with two generators was used to test T11. The fault was detected correctly on both generators, and detection was much faster than the one from the GPC.
- Detection of T12 occurred in the generator where a fault was introduced. Our detector was slower than the one from GPC. Also, our system was not able to detect the fault in the parallel (healthy) generator.

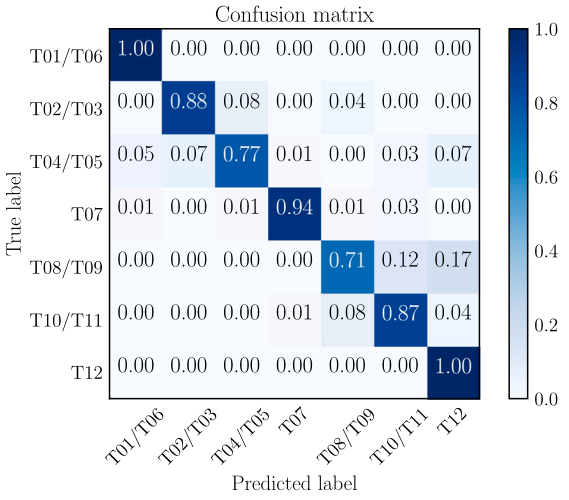

Fig. 4. Confusion matrix for classification of seven groups in Experiment 2.

5.2. Fault classification

The training for classification employed only data samples from faulty generators, and the testing was only considered after an alarm was triggered by the detection stage. We note that some faults have similar behavior, but are classified differently according to the cause of the fault. For instance, loss of voltage sensing for (T01) and partial loss of voltage sensing (T06) generate similar signals. Thus, five different experiments gathering faults into groups were devised for the fault classification problem.

Experiment 1. This experiment grouped all faults into only two classes: *AVR-related* faults (T01–T06) and *speed-related* faults (T07–T12). Fig. 3 shows the results when those two groups were considered separately. These results show that 96% of AVR-related fault samples were correctly classified as such, whereas practically all speed-related samples, considering round-offs, were correctly classified. These results represent average classification values along all samples and do not indicate a final post-processing result.

Experiment 2. In this case, the two classes considered in Experiment 1 were further split into seven more specialized classes: loss or voltage sensing (T01/T06), AVR operation (T02/T03), AVR oscillation-related (T04/T05), loss of speed sensing (T07), overproduction/underproduction (T08/T09), speed controller (T10/T11), and frozen fuel (T12) faults. Fig. 4 shows the confusion matrix considering the seven fault groups described above. In this experiment, classification hit rate was above 70% for all cases and above 86% for most cases.

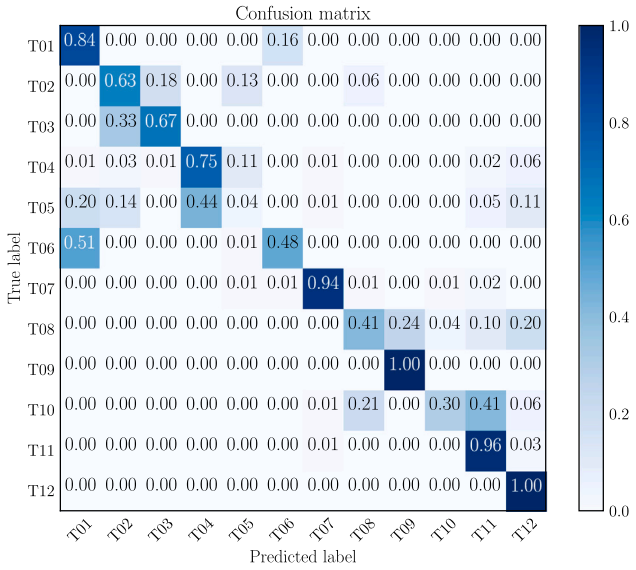

Fig. 5. Confusion matrix for classification of the 12 faults in Experiment 3.

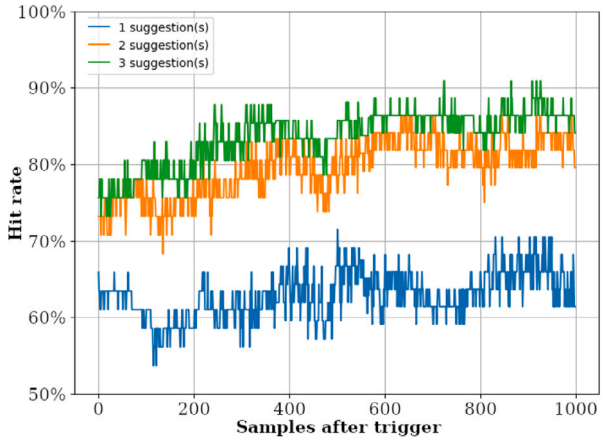

Fig. 6. Hit rate as a function of the number of samples after trigger. Results for $s = 1, 2, 3$ top probabilities in Experiment 4.

Experiment 3. In this experiment, all 12 faults were considered individually, constituting the most challenging classification case. Fig. 5 shows the classification results considering every fault individually. In this case, it is possible to observe that half of the faults (T01, T04, T07, T09, T11, and T12) were classified with probability larger than 70%, while some presented a considerable level of confusion due to similar behavior. Some examples include T01 and T06 (loss of voltage sensing), T02 and T03 (problems in the AVR operation), and T04 and T05 (AVR setup with bad configuration).

Experiment 4. In this last analysis, a simpler version of Experiment 3 was considered, where the classifier provided the one, two or three (s = 1, 2, or 3) most probable faults in a given situation. In a semi-supervised operational mode, an experienced human operator, based on his/her professional knowledge and on the information provided by the proposed system, might be able to identify the correct fault among these s possible alternatives. In order to test the classifier using the post-processing approach based on the RF output, we conducted a final temporal analysis of the hit rate. In this new experiment, if the actual fault type was among the s fault types with highest corresponding probabilities at the RF output, it was considered a hit. In Fig. 6 we considered the s highest probabilities among the RF-algorithm outputs, for $s = 1, 2, 3$. In this case, by increasing s the overall classification hit rate improves considerably, especially when one also increases the number of delay samples after trigger. Table 3 contains the hit rate per fault if classification was conducted 300 ms after the trigger instant. In cases where the proposed system was not able to *detect* faults and there was no trigger, the *onset* is used as reference. For 8 fault types, the hit rate is 100%, meaning that the correct classification was always among the $s = 3$ faults with highest probabilities. T02 (Internal AVR fault causing overexcitation) and T04 (Faulty voltage regulator — high gain causing oscillations) were correctly classified in half of the testing signals. T05 (Faulty voltage regulator — high derivation gain causing oscillations) was not among the top three at 300 ms for any of its testing signals. Note that all T01 cases are correct.

Table 3
Hit rate for a frame 300 ms after trigger or onset (in case of no trigger), considering the $s = 3$ highest probabilities in Experiment 4.

	Total signals	Detection issues	Hit rate (Trigger)	Hit rate (Onset)
T01	20	4 false alarms	100%	100%
T02	4		50%	
T03	2		100%	
T04	4		50%	
T05	2		0%	
T06	4		100%	
T07	2		100%	
T08	4	1 miss	100%	0%
T09	1		100%	
T10	4		100%	
T11	2		100%	
T12	2	1 miss	100%	100%

6. Conclusion

In this paper, a hybrid ML-based approach was proposed as an alternative for rule-based models to be employed in the detection and classification of faults in the power generation system of DP vessels. The proposed method is built upon experimental data that are representative of the fault cases considered, and for which the target labels (such as fault or not-fault) are known. The data and target labels are used to train the algorithm which, then, infers probabilities for labels on new and unlabeled data. This approach yields a fault-detection system independent of expert knowledge and of easy adaptation if new conditions are imposed on the data. Data were collected from a small-scale engine room and an analysis of the signals and corresponding features was presented in the paper. A pre-processing methodology based on PCA was employed to deal with high correlation between collected signals. Post-processing of the probability signal (output of the RF algorithm) for both fault detection and fault classification stages were also proposed and tested.

The proposed framework uses mostly ML blocks for detection and classification, but embeds a rule-based block in order to further improve results, given the limited availability of data. The system was tested on a portion of the data collected and results show improvement of detection speed and reliability, albeit presenting some false alarm cases, for 10 of 12 fault types considered, when compared against the rule-based model employed by the GPC. Two post-processing approaches were tested for classification: results for the first approach show that the system is able to classify reliably faults into similarity clusters. For the second approach, results show that the system infers with high probability the fault type.

CRediT authorship contribution statement

Igor M. Quintanilha: Equal responsibility in the conduction of the experiments, Writing - original draft. **Vitor R.M. Elias:** Equal responsibility in the conduction of the experiments, Writing - original draft. **Felipe B. da Silva:** Equal responsibility in the conduction of

the experiments, Writing - original draft. **Pedro A.M. Fonini:** Equal responsibility in the conduction of the experiments, Writing - original draft. **Eduardo A.B. da Silva:** Equal responsibility in the conduction of the experiments, Writing - original draft. **Sergio L. Netto:** Equal responsibility in the conduction of the experiments, Writing - original draft. **José A. Apolinário Jr.:** Equal responsibility in the conduction of the experiments, Writing - original draft. **Marcello L.R. de Campos:** Equal responsibility in the conduction of the experiments, Writing - original draft. **Wallace A. Martins:** Equal responsibility in the conduction of the experiments, Writing - original draft. **Lars E. Wold:** Equal responsibility in the conduction of the experiments, Writing - original draft. **Rune B. Andersen:** Equal responsibility in the conduction of the experiments, Writing - original draft.

Declaration of competing interest

The authors declare that they have no known competing financial interests or personal relationships that could have appeared to influence the work reported in this paper.

Acknowledgments

This work was financed by Siemens Norge AS, Norway, under contract UFRJ-COPPETEC PEE-20675, and also by the Coordenação de Aperfeiçoamento de Pessoal de Nível Superior – Brasil (CAPES) – Finance Code 001.

References

[1] Marine Contractors International Association. International guidelines for the safe operation of dynamically positioned offshore supply vessels. Tech. rep., London, UK: IMCA — The International Marine Contractors Association; 2015, p. 1–54.
[2] Johansen TA, Bø TI, Mathiesen E, Veksler A, Sørensen AJ. Dynamic positioning system as dynamic energy storage on diesel-electric ships. IEEE Trans Power Syst 2014;29(6):3086–91.
[3] Maritime Safety Committee. MSC/Circular.645 - guidelines for vessels with dynamic positioning systems. Tech. rep., The Maritime Safety Committee; 1994, p. 1–12.
[4] Shekhar C, Kumar A, Varshney S. Load sharing redundant repairable systems with switching and reboot delay. Reliab Eng Syst Saf 2020;193:106656.
[5] Niu G, Yang B-S, Pecht M. Development of an optimized condition-based maintenance system by data fusion and reliability-centered maintenance. Reliab Eng Syst Saf 2010;95(7):786–96.
[6] Cipollini F, Oneto L, Coraddu A, Murphy AJ, Anguita D. Condition-based maintenance of naval propulsion systems: Data analysis with minimal feedback. Reliab Eng Syst Saf 2018;177:12–23.
[7] Bae SJ, Mun BM, Chang W, Vidakovic B. Condition monitoring of a steam turbine generator using wavelet spectrum based control chart. Reliab Eng Syst Saf 2019;184:13–20.
[8] Wadi M, Baysal M, Shobole A. Comparison between open-ring and closed-ring grids reliability. In: 4th international conference on electrical and electronic engineering (ICEEE). Ankara, Turkey; 2017, p. 290–4.
[9] Andersen RB, Haukaas I. Challenges of protection and control system verification on DP3 vessels with focus on ride through fault and blackout. In: Dynamic positioning conference. Dynamic Positioning Committee — Marine Technology Society; 2013, p. 1–11.
[10] Kang HG, Jang S-C. Application of condition-based HRA method for a manual actuation of the safety features in a nuclear power plant. Reliab Eng Syst Saf 2006;91(6):627–33.
[11] Schaefer RC, Kim K. Excitation control of the synchronous generator. IEEE Ind Appl Mag 2001;7(2):37–43.
[12] Moura FAM, Camacho JR, Resende JW, Mendes WR. Synchronous generator, excitation and speed governor modeling in ATP-EMTP for interconnected DG Studies. In: 18th International conference on electrical machines. Wuhan, China; 2008, p. 1–6.
[13] Babaei M, Shi J, Abdelwahed S. A survey on fault detection, isolation, and reconfiguration methods in electric ship power systems. IEEE Access 2018;6:9430–41.
[14] Nandi S, Toliyat HA, Li X. Condition monitoring and fault diagnosis of electrical motors - a review. IEEE Trans Energy Convers 2005;20(4):719–29.
[15] Barik MA, Gargoom A, Mahmud MA, Haque ME, Al-Khalidi H, Than Oo AM. A decentralized fault detection technique for detecting single phase to ground faults in power distribution systems with resonant grounding. IEEE Trans Power Deliv 2018;33(5):2462–73.
[16] Mohanty SR, Pradhan AK, Routray A. A cumulative sum-based fault detector for power system relaying application. IEEE Trans Power Deliv 2008;23(1):79–86.
[17] Aldeen M, Sharma R. Robust detection of faults in frequency control loops. IEEE Trans Power Syst 2007;22(1):413–22.
[18] Yaghoubi M, Moghani JS, Noroozi N, Zolghadri MR. IGBT open-circuit fault diagnosis in a quasi-Z-Source Inverter. IEEE Trans Ind Electron 2018;1.
[19] Diniz PSR. Adaptive filtering: Algorithms and practical implementation. 4th ed.. New York, NY, USA: Springer; 2012.
[20] Jeong H, Park B, Park S, Min H, Lee S. Fault detection and identification method using observer-based residuals. Reliab Eng Syst Saf 2019;184:27–40.
[21] Dhoke A, Sharma R, Saha TK. An approach for fault detection and location in solar PV systems. Sol Energy 2019;194:197–208.
[22] Dhoke A, Sharma R, Saha TK. A technique for fault detection, identification and location in solar photovoltaic systems. Sol Energy 2020;206:864–74.
[23] Dustegor D, Poroseva SV, Hussaini MY, Woodruff S. Automated graph-based methodology for fault detection and location in power systems. IEEE Trans Power Deliv 2010;25(2):638–46.
[24] Pearson K. On lines and planes of closest fit to systems of points in space. Phil Mag 1901;2:559–72.
[25] Wang Y, Ma X, Qian P. Wind turbine fault detection and identification through PCA-based optimal variable selection. IEEE Trans Sustain Energy 2018;1.
[26] Avila NF, Figueroa G, Chu C. NTL detection in electric distribution systems using the maximal overlap discrete wavelet-packet transform and random undersampling boosting. IEEE Trans Power Syst 2018;33(6):7171–80.
[27] Rozenberg I, Beck Y, Eldar YC, Levron Y. Sparse estimation of faults by compressed sensing with structural constraints. IEEE Trans Power Syst 2018;33(6):5935–44.
[28] Chowdhury FN, Aravena JL. A modular methodology for fast fault detection and classification in power systems. IEEE Trans Control Syst Technol 1998;6(5):623–34.
[29] Moloi K, Hamam Y, Jordaan JA. Fault detection in power system integrated network with distribution generators using machine learning algorithms. In: 2019 6th international conference on soft computing machine intelligence (ISCMI). 2019, p. 18–22.
[30] Yang H, Liu X, Zhang D, Chen T, Li C, Huang W. Machine learning for power system protection and control. Electr J 2021;34(1):106881.
[31] Fazai R, Abodayeh K, Mansouri M, Trabelsi M, Nounou H, Nounou M, et al. Machine learning-based statistical testing hypothesis for fault detection in photovoltaic systems. Sol Energy 2019;190:405–13.
[32] Li W, Monti A, Ponci F. Fault detection and classification in medium voltage DC shipboard power systems with wavelets and artificial neural networks. IEEE Trans Instrum Meas 2014;63(11):2651–65.
[33] Liu S, Sun Y, Zhang L, Su P. Fault diagnosis of shipboard medium-voltage DC power system based on machine learning. Int J Electr Power Energy Syst 2021;124:106399.
[34] Yi Z, Etemadi AH. Line-to-line fault detection for photovoltaic arrays based on multiresolution signal decomposition and two-stage Support Vector Machine. IEEE Trans Ind Electron 2017;64(11):8546–56.
[35] Claudio M, Rocco S, Zio E. A support vector machine integrated system for the classification of operation anomalies in nuclear components and systems. Reliab Eng Syst Saf 2007;92(5):593–600.
[36] Kiranyaz S, Gastli A, Ben-Brahim L, Alemadi N, Gabbouj M. Real-time fault detection and identification for MMC using 1D convolutional neural networks. IEEE Trans Ind Electron 2018;1.
[37] Wen L, Li X, Gao L, Zhang Y. A new convolutional neural network-based data-driven fault diagnosis method. IEEE Trans Ind Electron 2018;65(7):5990–8.
[38] Nguyen KT, Medjaher K. A new dynamic predictive maintenance framework using deep learning for failure prognostics. Reliab Eng Syst Saf 2019;188:251–62.
[39] Zio E, Gola G. A neuro-fuzzy technique for fault diagnosis and its application to rotating machinery. Reliab Eng Syst Saf 2009;94(1):78–88.
[40] Li B, Delpha C, Diallo D, Migan-Dubois A. Application of artificial neural networks to photovoltaic fault detection and diagnosis: A review. Renew Sustain Energy Rev 2020;110512.
[41] Yu H, Khan F, Garaniya V. Risk-based fault detection using self-organizing map. Reliab Eng Syst Saf 2015;139:82–96.
[42] Breiman L. Random forests. Mach Learn 2001;45(1).
[43] Zhang D, Qian L, Mao B, Huang C, Huang B, Si Y. A data-driven design for fault detection of wind turbines using random forests and xgboost. IEEE Access 2018;6:21020–31.
[44] Zhou X, Lu P, Zheng Z, Tolliver D, Keramati A. Accident prediction accuracy assessment for highway-rail grade crossings using random forest algorithm compared with decision tree. Reliab Eng Syst Saf 2020;200:106931.
[45] Basurko OC, Uriondo Z. Condition-based maintenance for medium speed diesel engines used in vessels in operation. Appl Therm Eng 2015;80:404–12.
[46] Xia G, Liu T, Zhong W, Li J. Research on sensor fault diagnosis technology of dynamic positioning vessel based on filter and Support Vector Machine. In: 2017 IEEE international conference on mechatronics and automation (ICMA). Takamatsu, Japan; 2017, p. 1285–91.
[47] Bø TI, Dahl AR, Johansen TA, Mathiesen E, Miyazaki MR, Pedersen E, et al. Marine vessel and power plant system simulator. IEEE Access 2015;3:2065–79.

[48] Swider A, Pedersen E. Data-driven methodology for the analysis of operational profile and the quantification of electrical power variability on marine vessels. IEEE Trans Power Syst 2018. Early access.
[49] Settemsdal S, Radan D. DP3 class power system solutions for dynamically positioned vessels. In: Dynamic positioning conference. Dynamic Positioning Committee — Marine Technology Society; 2012, p. 1–33.
[50] Andersen RB, Haukaas I, Lund H, Tjong K, Zahedi B, Voreland S, et al. eSiLOOP™ DP3 vessels with hybrid power plant. In: Dynamic positioning conference. Dynamic Positioning Committee — Marine Technology Society; 2016, p. 1–26.
[51] Panda S, Sahu BK, Mohanty PK. Design and performance analysis of PID controller for an automatic voltage regulator system using simplified particle swarm optimization. J Franklin Inst B 2012;349(8):2609–25.
[52] Chatterjee S, Mukherjee V. PID controller for automatic voltage regulator using teaching-learning based optimization technique. Int J Electr Power Energy Syst 2016;77:418–29.
[53] Lee S, Yim J, Lee J, Sul S. Design of speed control loop of a variable speed diesel engine generator by electric governor. In: IEEE industry applications society annual meeting. Portland, OR, USA; 2008, p. 1–5.
[54] Louppe G. Understanding random forests: From theory to practice (Ph.D. Thesis), University of Liege, Belgium; 2014.
[55] Polikar R. Ensemble based systems in decision making. IEEE Circuits Syst Mag 2006;6(3):21–45.
[56] Gupta JD, Samanta S, Chanda B. Ensemble classifier-based off-line handwritten word recognition system in holistic approach. IET Image Process 2018;12(8):1467–74.
[57] Safavian SR, Landgrebe D. A survey of decision tree classifier methodology. IEEE Trans Syst Man Cybern 1991;21(3):660–74.
[58] Rutkowski L, Pietruczuk L, Duda P, Jaworski M. Decision trees for mining data streams based on the mcdiarmid's bound. IEEE Trans Knowl Data Eng 2013;25(6):1272–9.
[59] Yang Y, Morillo IG, Hospedales TM. Deep neural decision trees. In: ICML workshop on human interpretability in machine learning. Stockholm, Sweden; 2018, p. 34–40.
[60] Aich S, Younga K, Hui KL, Al-Absi AA, Sain M. A nonlinear decision tree based classification approach to predict the Parkinson's disease using different feature sets of voice data. In: 20th international conference on advanced communication technology (ICACT). Chuncheon Gang'weondo, South Korea; 2018, p. 638–42.
[61] IEEE standard common format for transient data exchange (COMTRADE) for power systems. IEEE Std C37.111-1999; 1999.
[62] Moore B. Principal component analysis in linear systems: Controllability, observability, and model reduction. IEEE Trans Automat Control 1981;26(1):17–32.
[63] Jiang Q, Yan X, Huang B. Performance-driven distributed PCA process monitoring based on fault-relevant variable selection and Bayesian inference. IEEE Trans Ind Electron 2016;63(1):377–86.
[64] Murphy KP. Machine learning: a probabilistic perspective. 1st ed.. Cambridge, MA, USA: MIT Press; 2013.
[65] Zadrozny B, Elkan C. Obtaining calibrated probability estimates from decision trees and naive Bayesian classifiers. In: Proceedings of the eighteenth international conference on machine learning. San Francisco, CA, USA; 2001, p. 609–16.
[66] Niculescu-Mizil A, Caruana R. Predicting good probabilities with supervised learning. In: Proceedings of the 22nd international conference on machine learning. Bonn, Germany; 2005, p. 625–32.
[67] Kull M, Silva Filho TM, Flach P. Beyond sigmoids: How to obtain well-calibrated probabilities from binary classifiers with beta calibration. Electron J Stat 2017;11(2):5052–80.
[68] Cohen J. A coefficient of agreement for nominal scales. Educ Psychol Meas 1960;20(1):37–46.